gradients close to the air–water interface, where veils develop within a few minutes. A suspension of latex beads (1 or 0.5 μm) was then added with a capillary pipette. Preparations were recorded with dark-field illumination using a CCD camera (Sony) attached to the microscope and a video recorder. Afterwards, positions of individual latex beads were recorded frame by frame (at 0.04-s intervals). Only trajectories that were almost parallel to the plane of observation were included.

Oxygen gradients. Oxygen microelectrodes (with a 5–10-μm tip)[3] connected to a picoammeter were mounted in a micromanipulator. The surface of the *Thiovulum* veil and the electrode tip were observed through a dissection microscope tilted at an angle of 45°; this made it possible to map the O_2 isopleths inside and above the veil. Microelectrodes penetrating from above tend to deform the O_2 diffusion gradients above the sediment[14], but this should not affect the relative position of O_2 isopleths in different areas of the veil. The fact that O_2 was measured in a vertical convective flow is also likely to minimize this effect.

Received 27 January; accepted 8 May 1998.

1. Purcell, E. M. Life at low Reynolds number. *Am. J. Phys.* **45,** 3–11 (1977).
2. Revsbech, N. P., Jørgensen, B. B. & Blackburn, T. H. Oxygen in the sea bottom measured with a microelectrode. *Science* **207,** 1355–1356 (1980).
3. Revsbech, N. P. & Jøgensen, B. B. Microelectrodes: their use in microbial ecology. *Adv. Microbiol. Ecol.* **9,** 293–352 (1986).
4. Wirsen, C. O. & Jannasch, H. W. Physiological and morphological observations on *Thiovulum* sp. *J. Bacteriol.* **136,** 765–774 (1978).
5. Garcia-Pichel, F. Rapid bacterial swimming measured in swarming cells of *Thiovulum majus*. *J. Bacteriol.* **171,** 3560–3563 (1989).
6. Fenchel, T. Motility and chemosensory behaviour of the sulphur bacterium *Thiovulum majus*. *Microbiology* **140,** 3109–3116 (1994).
7. Jørgensen, B. B. & Revsbech, N. P. Colorless sulfur bacteria, *Beggiatoa* spp. and *Thiovulum* spp. in O_2 and H_2S microgradients. *Appl. Environ. Microbiol.* **45,** 1261–1270 (1983).
8. Lighthill, J. Flagellar hydrodynamics. *Soc. Indust. Appl. Math. Rev.* **18,** 161–230 (1976).
9. Vogel, S. *Life in moving fluids* (Grant, Boston, 1981).
10. Fenchel, T. & Bernard, C. Mats of colourless sulphur bacteria. I Major microbial processes. *Mar. Ecol. Prog. Ser.* **128,** 161–170 (1995).
11. Aller, R. C. & Yingst, J. Y. Effects of marine deposit-feeders *Heteromastus filiformis* (Polychaeta), *Macoma balthica* (Bivalvia), and *Tellina texana* (Bivalvia) on averaged solute transport, reaction rates, and microbial distributions. *J. Mar. Res.* **41,** 299–322 (1985).
12. Dando, P. R. *et al*. The effects of methane seepage at an intertidal/shallow subtidal site on the shore of Kattegat, Vendsyssel. *Bull. Geol. Soc. Denmark* **41,** 65–79 (1994).
13. Gundersen, J. K., Jørgensen, B. B., Larsen, E. & Jannasch, H. W. Mats of giant sulphur bacteria on deep-sea sediments due to fluctuating hydrothermal flow. *Nature* **360,** 454–455 (1992).
14. Glud, R. N., Gundersen, J. K., Revsbech, N. P. & Jørgensen, B. B. Effects on the benthic diffusive boundary layer imposed by microelectrodes. *Limnol. Oceanogr.* **39,** 462–467 (1994).

Acknowledgements. We thank J. Johansen for technical assistance. This study was supported by grants from the Danish Natural Science Research Council.

Correspondence and requests for materials should be addressed to T.F. (e-mail: mbltf@inet.uni2.dk).

Full-term development of mice from enucleated oocytes injected with cumulus cell nuclei

T. Wakayama*†, A. C. F. Perry*‡, M. Zuccotti*§, K. R. Johnson‖ & R. Yanagimachi*

** Department of Anatomy and Reproductive Biology, John A. Burns School of Medicine, University of Hawaii, Honolulu, Hawaii 96822, USA*
† Department of Veterinary Anatomy, Faculty of Agriculture, University of Tokyo, Bunkyo-ku, Tokyo 113, Japan
‡ Department of Signalling, Babraham Institute, Cambridge CB2 4AT, UK
§ Dipartimento Biologia Animale, Laboratorio Biologia dello Sviluppo, University of Pavia, Piazza Botta 10, 27100, Pavia, Italy
‖ Jackson Laboratory, 600 Main Street, Bar Harbor, Maine 04609, USA

Until recently, fertilization was the only way to produce viable mammalian offspring, a process implicitly involving male and female gametes. However, techniques involving fusion of embryonic or fetal somatic cells with enucleated oocytes have become steadily more successful in generating cloned young[1–3]. Dolly the sheep[4] was produced by electrofusion of sheep mammary-derived cells with enucleated sheep oocytes. Here we investigate the factors governing embryonic development by introducing nuclei from somatic cells (Sertoli, neuronal and cumulus cells) taken from adult mice into enucleated mouse oocytes. We found that some enucleated oocytes receiving Sertoli or neuronal nuclei developed *in vitro* and implanted following transfer, but none developed beyond 8.5 days post coitum; however, a high percentage of enucleated oocytes receiving cumulus nuclei developed *in vitro*. Once transferred, many of these embryos implanted and, although most were subsequently resorbed, a significant proportion (2 to 2.8%) developed to term. These experiments show that for mammals, nuclei from terminally differentiated, adult somatic cells of known phenotype introduced into enucleated oocytes are capable of supporting full development.

Previous studies have suggested that embryonic development is enhanced when donor nuclei are in the G0 or G1 phase of the cell cycle[1,3,4], and Dolly the sheep developed from an enucleated oocyte electrofused with a mammary-derived cell presumed to be in G0 following culture in serum-deficient medium for 5 days[4]. We have investigated the developmental potential of oocytes injected with the nuclei of non-cultured cells known to be at G0. We selected

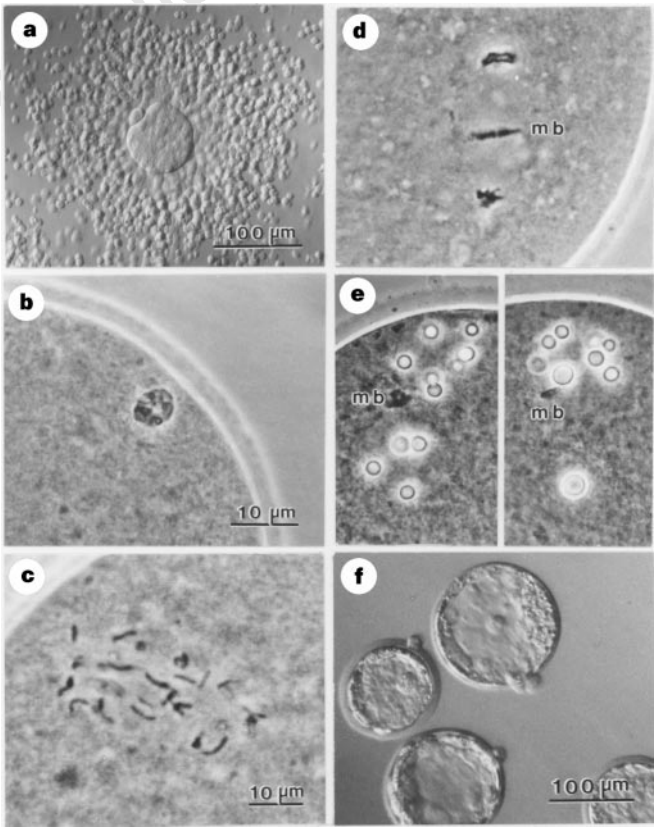

Figure 1 *In vitro* development of enucleated oocytes following injection of cumulus cell nuclei. **a**, Live oocyte surrounded by cumulus cells. The egg coat (the zona pellucida) appears in this micrograph as a relatively clear zone around the oocyte. **b**–**e**, Behaviour of cumulus cell nuclei following injection into enucleated oocytes, photographed after fixation and staining. **b**, A cumulus cell nucleus within 10 min of injection. **c**, Transformation of the nucleus into disarrayed chromosomes 3 h after injection. The disorder reflects an unusual situation in which single, condensed chromatids are each attached to a single pole of the spindle and are therefore not aligned on a metaphase plate. **d**, 1 h after Sr^{2+} activation, chromosomes are segregated into two groups (mb, midbody). **e**, 5 h after Sr^{2+} activation, two pseudo-pronuclei (left and right panels) with a varying number of distinct nucleolus-like structures are discernible in each egg. The size and number of pseudo-pronuclei varied, suggesting that segregation of chromosomes was random after oocyte activation. **f**, Live blastocysts produced following injection of enucleated oocytes with cumulus cell nuclei.

Table 1 Preimplantation of enucleated eggs injected with cumulus cell nuclei

Time of oocyte activation	Total no. of oocytes used	No. of enucleated oocytes	No. of surviving oocytes after injection	No. (%) of activated oocytes	No. (%, mean ± s.d.) of embryos developed from oocytes at 72 h after activation		
					1-cell and abnormal	2–8-cell	Morula/blastocyst*
Simultaneously with injection	233	230	182	153 (84.1)	17	75	61 (39.9 ± 16.6)
1–3 h after injection	573	565	508	474 (93.3)	20	177	277 (58.4 ± 12.6)
3–6 h after injection	195	191	182	151 (83.0)	9	41	101 (66.9 ± 14.4)

* There is a significant different ($P < 0.005$) between the top result and the bottom two. Data were analysed using the χ^2 test.

Sertoli, neuronal and cumulus from adult mice as representatives of this class; Sertoli cells and neurons do not normally divide in adults but remain at G0, and more than 90% of cumulus cells surrounding recently ovulated oocytes (Fig. 1a) are in the G0/G1 phase of the cell cycle[5]. These somatic cell types have very distinctive morphologies, making them easy to identify with confidence. All cells were used immediately (that is, without *in vitro* culturing) following the removal of tissue from freshly killed mice.

Enucleated mouse oocytes were each injected with a single nucleus from one of the three somatic cell types and left for 0 to 6 hours before activation. Examination of enucleated oocytes injected with cumulus nuclei revealed that chromosome condensation had occurred within 1 hour of injection (Fig. 1b, c). When, after 1 to 6 hours incubation, oocytes were activated in culture medium containing Sr^{2+} and cytochalasin B, their cumulus-derived chromosomes segregated (Fig. 1d) to form structures resembling the pronuclei that are formed after normal fertilization (referred to here as pseudo-pronuclei). Examination of 47 such oocytes after fixation and staining showed that 64% had two pseudo-pronuclei (Fig. 1e) and 36% had three or more. Oocytes with distinct pseudo-pronuclei were considered to be activated. Owing to the cytokinesis-blocking effect of cytochalasin B, no polar body was formed and therefore all chromosomes were retained within the oocyte, regardless of the number of pseudo-pronuclei. Chromosome analysis of 13 such oocytes fixed before the first cleavage (data not shown) revealed that 85% had a normal total chromosome number ($2n = 40$). The time interval between nucleus injection and oocyte activation appeared to affect the rate of oocyte development (Table 1). Activation immediately after nucleus injection led to

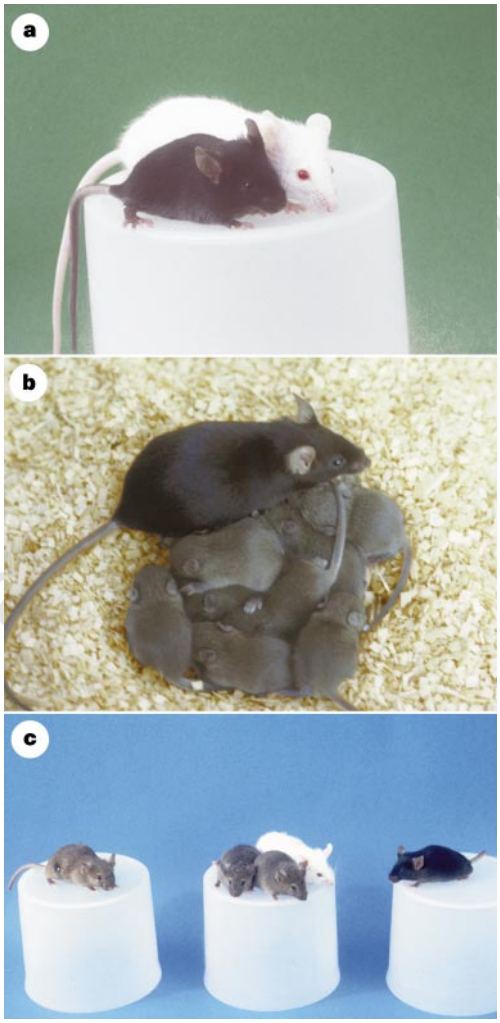

Figure 2 Cloned mice. **a**, The first surviving cloned mouse, Cumulina (born 3 October 1997) at four weeks (foreground) with her foster mother. **b**, Cumulina at 2.5 months with the pups she produced following mating with a CD-1 (albino) male. **c**, Two B6C3F1-derived, cloned, agouti young (centre) in front of their albino foster mother (CD-1), and a B6D2F1 oocyte donor (black, right). The two agouti offspring in the centre are clones (identical 'twin' sisters) of the agouti B6C3F1 cumulus donor shown on the left, and are two of the offspring described in series C (see text) and Table 2.

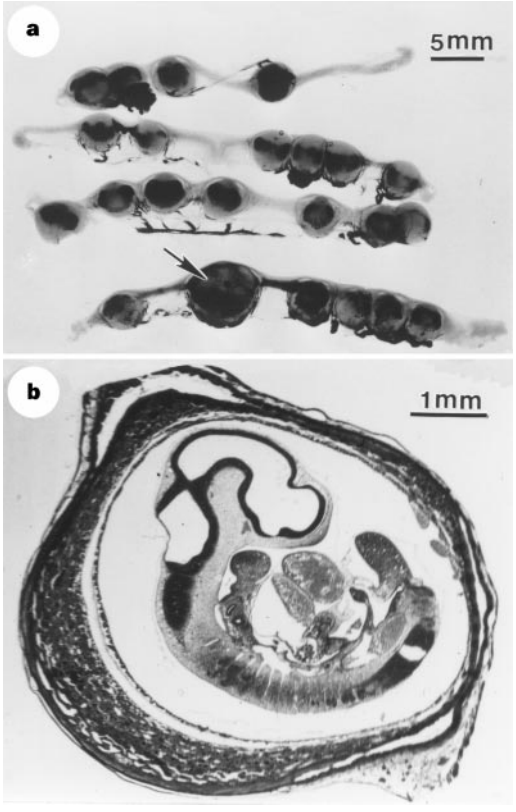

Figure 3 Development following uterine transfer of embryos produced after injection of Sertoli cell nuclei into enucleated oocytes. **a**, Uteri of recipient females 8.5 d.p.c., fixed with Bouin's fluid, dehydrated and cleared with benzyl benzoate. All uterine implantation sites failed to develop except for one (arrow), in which an embryo (**b**) appeared to be normal and was at the ~12-somite stage.

Table 2 Development of enucleated eggs injected with Sertoli or brain-cell nuclei*

Cell type injected	No. of surviving oocytes injected	No. (%) of oocytes activated	Total no. (%) of morulae/blastocysts developed†	No. of transferred embryos (recipients)	No. (%) of implantation sites	No. (%) of fetuses
Sertoli	159	159 (100)	63 (39.6)	59 (8)	41 (69.5)	1 (1.7)
Brain	228	223 (97.8)	50 (22.4)	46 (5)	25 (54.3)	1 (2.2)‡

* All recipients were killed at 8.5 d.p.c.
† There is a significant difference ($P < 0.005$) between the top and bottom result.
‡ Died at about 6–7 d.p.c.

significantly poorer development to morulae/blastocysts *in vitro* (Fig. 1f) than was achieved when activation followed a delay of 1 to 6 hours.

On the basis of this information, we injected Sertoli and neuronal nuclei into enucleated oocytes and delayed activation for 1 to 6 hours: about 40% of enucleated oocytes that had been injected with Sertoli cell nuclei, and 22% of those injected with neuronal nuclei, developed into morulae/blastocysts *in vitro* (Table 2). As these values were less than those achieved after cumulus nucleus injection (58–67%; Table 1), we concentrated on the potential of cumulus cell nuclei to support embryonic development *in vivo*.

In the first series of experiments (series A in Table 3), a total of 142 developing embryos (at the 2-cell to blastocyst stage) were transferred to 16 recipient females. When these females were examined at 8.5 and 11.5 d.p.c., 5 live and 5 dead fetuses were seen *in uteri*. In the second series (series B in Table 3), a total of 800 embryos were transferred into 54 foster mothers, and caesarean sections at 18.5–19.5 d.p.c. revealed 17 live fetuses. Of these, six died soon after delivery, one died approximately 7 days after delivery, but the remaining ten females survived and are apparently healthy. All of these, including the first-born survivor (born on 3 October 1997 and named 'Cumulina'; Fig. 2a), have been mated and have delivered and raised normal offspring (Fig. 2b). Several of these offspring have, in turn, now developed into fertile adults.

In the third series of experiments (series C in Table 3), B6C3F1 mice carry a copy of the *agouti* (*A*) gene, and are consequently agouti; offspring from this experiment should therefore have an agouti coat colour, rather than the black of the B6D2F1 oocyte donors. A total of 298 embryos derived from B6C3F1 cumulus cell nuclei were transferred to 18 foster mothers. Caesarean sections at 19.5 d.p.c. revealed six live fetuses whose placentas were used in DNA-typing analysis. Although one died a day after birth, the five extant females are healthy and have the agouti coat phenotype. Figure 2c shows two such agouti pups with their albino foster mother (CD-1).

We did additional experiments (series D in Table 3) to investigate whether clones could be more efficiently cloned in subsequent rounds of recloning. We therefore collected cumulus cells from B6C3F1 (agouti) clones generated in series C and injected their nuclei into enucleated B6D2F1 oocytes to generate embryos that were transferred as described for series B and C. A total of 287 embryos derived from cloned B6C3F1 cumulus-cell nuclei were transferred to 18 foster mothers. When caesarean sections were done at 19.5 d.p.c. eight live fetuses were recovered. Although one died soon after birth, the seven surviving females are healthy and have the predicted agouti coat phenotype. These results indicate that clones (series B and C) and cloned clones (series D) are produced with comparable efficiency. This argues that successive generations of clones do not undergo changes (either positive or negative) that influence the outcome of the cloning process.

We also monitored the developmental potential *in vivo* of morulae/blastocysts generated following the injection of either Sertoli-cell or neuronal nuclei into enucleated oocytes (all cells from non-clones) (Table 2). Embryos produced by Sertoli-nucleus injection resulted in a single live fetus (Fig. 3) in the uterus of a foster mother killed 8.5 d.p.c. (Table 2). We failed to detect *in vivo* development of embryos derived following injection of neuronal nuclei beyond 6–7 d.p.c.

We believe that all of the live offspring reported here represent clones derived from cumulus-cell nuclei in the absence of genetic

Table 3 Postimplantation development of enucleated eggs injected with cumulus cell nuclei

Experiment series*	Time of oocyte activation	No. of injected oocytes	No. of transferred embryos (recipients)	No. (%) of implantations from transferred embryos†	No. of fetuses developed from transferred embryos					No. (%) of newborn from transferred embryos
					Total (%)†	8.5 d.p.c.		11.5 d.p.c.		
						Live	Dead	Live	Dead	
A	Simultaneously with injection	82	34 (4)	8 (23.5)	0					–
	1–3 h after injection	136	45 (5)	32 (71.1)	7 (15.6)	3	2‡	2	0	–
	3–6 h after injection	124	63 (7)	36 (57.1)	3 (4.8)	0	2§	0	1‖	–
B	1–3 h after injection	1345	760 (49)	–	–	–	–	–	–	16 (2.1)
	3–6 h after injection	62	40 (5)	–	–	–	–	–	–	1 (2.5)
C	1–3 h after injection	458	298 (18)	–	–	–	–	–	–	6 (2.0)
D	1–3 h after injection	603	287 (18)	–	–	–	–	–	–	8 (2.8)

* Series A, caesarean sections were done at 8.5 or 11.5 d.p.c.; series B and C, caesarean sections were done at 18.5–19.5 d.p.c. In series A and B, each donor nucleus is from a B6D2F1 cumulus cells; in series C, each donor nucleus is from a B6C3F1 cumulus cell; in series D, each donor nucleus is from a B6C3F1 clones mouse from series C.
† There is a significant difference between the top result and the bottom two: implantation ($P < 0.005$); fetal development ($P < 0.05$). Data were analysed by χ^2 tests.
‡ Died 6–7 d.p.c.
§ Died 7–8 d.p.c.
‖ Died 10 d.p.c.

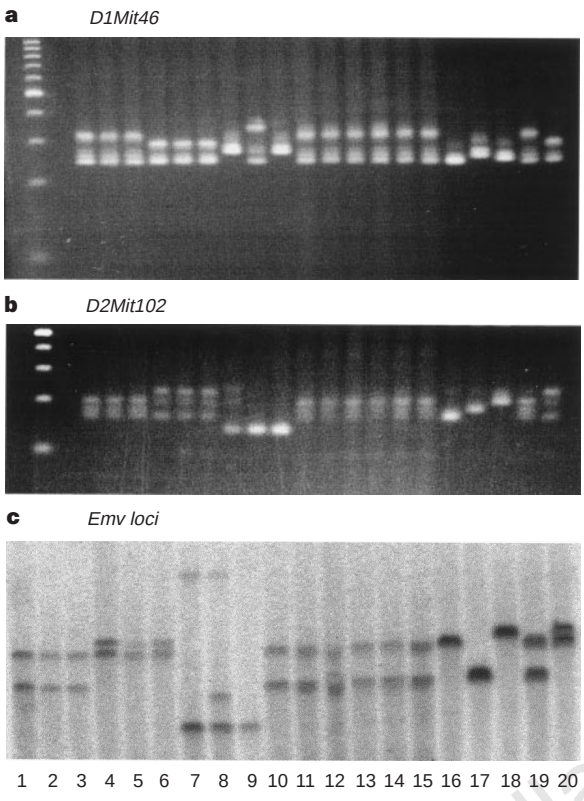

Figure 4 DNA typing of donors and offspring in series C corroborates the genetic identify of the cloned offspring to cumulus cell donors, and non-identity to oocyte donors and host foster females. **a**, PCR typing using the strain-specific marker *D1Mit46*. **b**, PCR -amplified DNA (**a**, **b**) from F_1 hybrid mice gives an additional gel band not seen in the DNA from inbred parental strains (lanes 16–20); this extra band corresponds to a heteroduplex derived from the two parental products, whose conformation results in anomolous gel migration. **c**, Southern blot typing of strain-specific *Emv* loci (*Emv1*, *Emv2* and *Emv3*). Placental DNA from the six cloned series C offspring (lanes 10–15) was compared with DNA from the three cumulus cell donor females (lanes 1–3), the three oocyte recipient females (lanes 4–6), and the three host females (lanes 7–9). Control DNA was from C57BL/6 (lane 16), C3H (lane 17), DBA/2 (lane 18), B6C3F1 (lane 19) or B6D2F1 (lane 20). 100-bp DNA size-marker ladders are shown on the left of **a** and **b**.

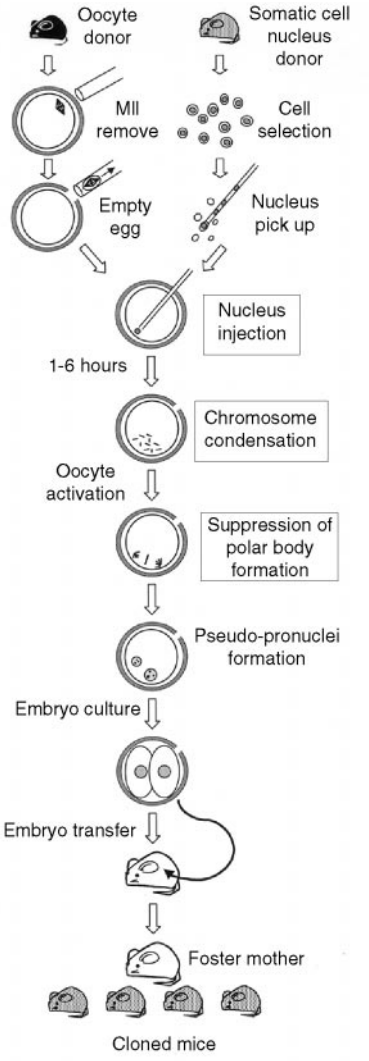

Figure 5 The cloning procedure developed here, as described in the text and Methods section.

contamination, for the following reasons. (1) Oocytes/eggs were not exposed to spermatozoa *in vitro*. (2) Foster mothers (CD-1, albino) were mated with vasectomized males (CD-1, albino) of established infertility. In the unlikely event of fertilization by such a vasectomized male, the offspring would be albino. We transferred 2- to 8-cell embryos/blastocysts into the oviducts/uteri of foster mothers; it is well established that 2- to 8-cell mouse embryos/blastocysts cannot be fertilized by spermatozoa[6]. (3) All full-term animals were born with black eyes; the surviving ten from series B have black coats and the surviving five in series C have agouti coats. This pattern of coat colour inheritance exactly matches that predicted by the genotype of the nucleus donor in each case. As B6D2F1 mice lack the *agouti* gene, the agouti mice in series C must have inherited their agouti coat colour from a non-B6D2F1 nucleus. (4) Where possible, all putative clones have been sexed, and all were found to be females, consistent with their genetic progenitors invariably being female. (5) DNA typing of highly variable alleles diagnostic of the B6, C3, D2 and CD-1 strains used here (Fig. 4) demonstrates beyond reasonable doubt that the six cloned offspring in series C (which includes one that died soon after birth) are isogenic with the three cumulus cell donor females used (B6C3F1) and do not contain DNA derived from either the oocyte donors (B6D2F1) or host foster mothers (CD-1). (6) Following enucleation, we suppressed extrusion of chromosomes into polar bodies using cytochalasin B. Thus, even if enucleation of the oocytes had been either totally unsuccessful or only partly successful, all resulting zygotes would be hyperploid; such embryos are inviable and cannot develop into normal offspring[7]. Moreover, in mock experiments, we enucleated 204 oocytes and examined them after fixation and staining[8]: no chromosomes were apparent, suggesting that the efficiency of chromosome removal exceeded 99.99%.

In general, nuclei have previously been transferred either into enucleated, one-cell embryos[9], or into unfertilized, enucleated oocytes[10,11] which were then immediately activated, thereby preventing chromosome condensation[12]. Mouse embryonic stem[13] or primordial germ[14] cell nuclei transferred into enucleated oocytes that were then immediately activated produced embryos capable of developing to blastocysts, with a minority of these implanting. In contrast, activation that was delayed for 30 to 60 minutes after the introduction of thymocyte nuclei into enucleated oocytes[15] often resulted in the extrusion of a pseudo-polar body, with a consequently high incidence of hypoaneuploidy (78%) and with none of the embryos developing beyond the 4-cell stage.

We have shown that a relatively high proportion of enucleated oocytes can develop to morulae/blastocysts and beyond when they are activated after a prolonged delay following injection of adult-

derived, somatic cell nuclei. Indeed, the inclusion of a prolonged interval between nuclear injection and oocyte activation (and suppression of cytokinesis) was apparently beneficial for both pre- and post-implantation development (Tables 1, 3). Although this seems paradoxical after earlier work, prolonged exposure of incoming nuclei to a cytoplasm rich in metaphase promoting factor causes persistent chromosome condensation (in the absence of DNA synthesis) and may facilitate the nuclear changes that are essential for development. We are studying the molecular events attending this latent period with respect to potential epigenetic 'reprogramming' and chromatin repair, *inter alia*. Also, the use of a piezo-impact pipette drive unit[16,17] may have contributed to a high rate of embryonic development by enabling oocyte and donor nucleus manipulation to be quick and efficient, thereby reducing the trauma to both in comparison with methods using electrofusion, Sendai virus or polyethylene glycol. Furthermore, we minimized the amount of somatic cell cytoplasm introduced into enucleated oocytes, which might otherwise have interfered with the onset of development.

It is unclear why Sertoli and neuronal cell nuclei failed to produce full-term embryos. Although our study does not preclude the possibility that these nuclei (and nuclei from other cell types) may be able to support full-term development, this finding suggests that the G0 status of donor nuclei is not sufficient *per se* to ensure embryonic development. We did not use mural granulosa cells, which differ functionally and in their subsequent fate from cumulus cells[18], and the question is open as to whether their nuclei might prime embryonic development to term. The contrastingly high implantation rate (57–71%) and low fetal (5–16%) and full-term (2–3%) developmental rates (Table 3) indicate that several regulatory morphogenic factors and checkpoints may be involved in the development of post-implantation embryos/fetuses.

Our results suggest that, contrary to previous opinion[9], mammals can be reproducibly cloned from adult somatic cells. Furthermore, we believe that the success of these experiments in the mouse provides an amenable model with which to evaluate the molecular mechanisms that regulate the reprogramming of somatic cell genomes, genomic imprinting, embryonic genome activation and cell differentiation. □

Methods

The cloning procedure is summarized in Fig. 5.

Isolation of cumulus cells. Female B6D2F1 (C57BL/6 × DBA/2 used in series A and B), B6C3F1 (C57BL/6 × C3H/He used in series C) or B6C3F1 clones produced in series C were induced to superovulate by consecutive injection of eCG and hCG. 13 h after hCG injection, cumulus–oocyte complexes were collected from oviducts and treated in HEPES–CZB medium[19] supplemented with bovine testicular hyaluronidase (0.1% (w/v), 300 U mg^{-1}) to disperse cumulus cells. We selected cumulus cells of modal (>70%) diameter (10–12 μm) for injection. From preliminary experiments, nuclei from cells with smaller or larger diameters (8–9 or 13–15 μm, respectively) seldom supported development of injected eggs beyond the 8-cell stage (data not shown). Following dispersal, cells were transferred to HEPES–CZB containing 10% (w/v) polyvinylpyrrolidone (average M_r, 360,000) and kept at room temperature for up to 3 h before injection.

Isolation of Sertoli cells and neurons. Sertoli cells were isolated from the testes of 6-month-old B6D2F1 males as described[20], except that HEPES–Ham F-12 medium was used. Manipulation of individual Sertoli cells was done by using a large injection pipette (inner diameter ~10 μm). Neuronal cells were isolated from the cerebral cortex of adult B6D2F1 females. Brain tissue was removed with sterile scissors, quickly washed in erythrocyte-lysing buffer and gently hand-homogenized for several seconds in nucleus isolation medium[21] at room temperature. Nuclei (7–8 μm in diameter) harbouring a conspicuous nucleolus were individually collected from the resulting suspension using the injection pipette before delivery into a recipient enucleated oocyte.

Enucleation of metaphase II oocytes and donor cell nucleus injection. B6D2F1 oocytes (obtained 13 h after hCG injection of eCG-primed females) were freed from the cumulus oophorous and held in CZB medium at 37.5 °C under 5% (v/v) CO_2 in air until required. Groups of oocytes (usually 10–15) were transferred into a droplet of HEPES–CZB containing 5 μg ml^{-1} cytochalasin B, which had previously been placed in the operation chamber on the microscope stage. Oocytes undergoing microsurgery were held with a holding pipette and the zona pellucida 'cored' following the application of several piezo-pulses to an enucleation pipette. The metaphase II chromosome–spindle complex (identifiable as a translucent region) was aspirated into the pipette with a minimal volume of oocyte cytoplasm[22]. After enucleation of all oocytes in one group (~10 min), they were transferred into cytochalasin B-free CZB and held there for up to 2 h at 37.5 °C, then returned to the microscope stage immediately before further manipulation. Nuclei were removed from their respective somatic cells and gently aspirated in and out of the injection pipette (~7 μm inner diameter) until their nuclei were largely devoid of visible cytoplasmic material. Each nucleus was injected into a separate enucleated oocyte within 5 min of its isolation as described[17].

Oocyte activation. Following somatic-cell nucleus injection, some groups of oocytes were placed immediately in Ca^{2+}-free CZB containing both 10 mM Sr^{2+} and 5 μg ml^{-1} cytochalasin B for 6 h. Additional groups of enucleated oocytes injected with cumulus cell nuclei were left in CZB medium at 37.5 °C under 5% (v/v) CO_2 in air for 1–6 h before activation by Sr^{2+} in the presence of 5 μg ml^{-1} cytochalasin B. Sr^{2+} treatment activated the oocytes[23], whereas cytochalasin B prevented subsequent polar-body formation and therefore chromosome expulsion. Following activation, all resulting embryos were transferred to Sr^{2+}-free, cytochalasin B-free CZB medium and incubation was continued at 37.5 °C under 5% (v/v) CO_2 in air.

Embryo transfer. Where appropriate, 2- to 8-cell embryos or morulae/blastocysts were respectively transferred into oviducts or uteri of foster mothers (CD-1, albino) that had been mated with vasectomized CD-1 males 1 or 3 days previously. Following caesarean section of recipient females at 18.5–19.5 d.p.c., live young were raised by lactating CD-1 foster mothers.

DNA typing. DNA from the following control strains and hybrids was obtained from spleen tissue: C57BL/6J (B6), C3H/HeJ (C3), DBA/2J (D2), B6C3F1 and B6D2F1. DNA from the three cumulus cell donor females (B6C3F1), the three oocyte recipient females (B6D2F1) and the three foster females (CD-1) was prepared from tail-tip biopsies. DNA from the six B6C3F1-derived, cloned offspring was prepared from their associated placentas. For the microsatellite markers *D1Mit46*, *D2Mit102* and *D3Mit49*, primer pairs (MapPairs) were purchased from Research Genetics and typed as described[24], except that PCR was carried out for 30 cycles and products were separated by 3% agarose gels (Metaphor) and visualized by ethidium bromide staining. Endogenous ecotropic murine leukaemia provirus DNA sequences (*Emv* loci) were identified following hybridization of *Pvu*II-digested genomic DNA to the diagnostic probe, pEc-B4 (ref. 25). Probe labelling, Southern blotting and hybridization procedures have been described[26].

Received 23 December 1997; accepted 19 June 1998.

1. Campbell, K. H. S., Loi, P., Otaegui, P. J. & Wilmut, I. Cell cycle co-ordination in embryo cloning by nuclear transfer. *Rev. Reprod.* **1,** 40–45 (1996).
2. Kono, T. Nuclear transfer and reprogramming. *Rev. Reprod.* **2,** 74–80 (1997).
3. Campbell, K. H. S., McWhir, J., Ritchie, W. A. & Wilmut, I. Sheep cloned by nuclear transfer from a cultured cell line. *Nature* **380,** 64–66 (1996).
4. Wilmut, I., Schnieke, A. E., McWhir, J., Kind, A. J. & Campbell, K. H. S. Viable offspring derived from fetal and adult mammalian cells. *Nature* **385,** 810–813 (1997).
5. Schuetz, A. W., Whittingham, D. G. & Snowden, R. Alterations in the cell cycle of mouse cumulus granulosa cells during expansion and mucification *in vivo* and *in vitro*. *Reprod. Fertil. Dev.* **8,** 935–943 (1996).
6. Wassarman, P. The biology and chemistry of fertilization. *Science* **235,** 553–560 (1987).
7. Epstein, C. J. *The Consequences of Chromosome Imbalance* (Cambridge University Press, 1986).
8. Yanagida, K., Yanagimachi, R., Perreault, S. D. & Kleinfeld, R. G. Thermostabiity of sperm nuclei assessed by microinjection into hamster oocytes. *Biol. Reprod.* **44,** 440–447 (1991).
9. McGrath, J. & Solter, D. Inability of mouse blastmere nuclei transferred to enucleated zygotes to support development *in vitro*. *Science* **226,** 1317–1319 (1984).
10. Willadsen, S. M. Nuclear transplantation in sheep embryos. *Nature* **320,** 63–65 (1986).
11. Collas, P. & Barnes, F. L. Nuclear transplantation by microinjection of inner cell mass and granulosa cell nuclei. *Mol. Reprod. Dev.* **38,** 264–267 (1994).
12. Czolowska, R., Modlinski, J. A. & Tarkowski, A. K. Behavior of thymocyte nuclei in non-activated and activated mouse oocytes. *J. Cell Sci.* **69,** 19–34 (1984).
13. Tsunoda, T. & Kato, Y. Nuclear transplantation of embryonic stem cells in mice. *J. Reprod. Fertil.* **98,** 537–540 (1993).
14. Tsunoda, T., Tokunaga, T., Imai, I. & Uchida, T. Nuclear transplantation of male primordial germ cells in the mouse. *Development* **107,** 407–411 (1989).
15. Kono, T., Ogawa, M. & Nakahara, T. Thymocyte transfer to enucleated oocytes in the mouse. *J. Reprod. Dev.* **39,** 301–307 (1993).
16. Kimura, Y. & Yanagimachi, R. Intracytoplasmic sperm injection in the mouse. *Biol. Reprod.* **52,** 709–720 (1995).

17. Kimura, Y. & Yanagimachi, R. Mouse oocytes injected with testicular spermatozoa or round spermatids can develop into normal offspring. *Development* **121,** 2397–2405 (1995).
18. Eppig, J., Wigglesworth, K., Pendola, F. & Hirao, Y. Murine oocytes suppress expression of luteinizing hormone receptor messenger ribonucleic acid by granulosa cells. *Biol. Reprod.* **56,** 976–984 (1997).
19. Chatot, C. L., Lewis, J. L., Torres, I. & Ziomek, C. A. Development of 1-cell embryos from different strains of mice in CZB medium. *Biol. Reprod.* **42,** 432–440 (1990).
20. Erickson, R. P., Zwigman, T. & Ao, A. Gene expression, X-inactivation, and methylation during spermatogenesis: the case of *Zfa*, *Zfx* and *Zfy* in mice. *Mol. Reprod. Dev.* **35,** 114–120 (1993).
21. Kuretake, S., Kimura, Y., Hoshi, K. & Yanagimachi, R. Fertilization and development of mouse oocytes injected with isolated sperm heads. *Biol. Reprod.* **55,** 789–795 (1996).
22. Kono, T., Sotomaru, Y., Sato, Y. & Nakahara, T. Development of androgenetic mouse embryos produced by *in vitro* fertilization of enucleated oocytes. *Mol. Reprod. Dev.* **34,** 43–46 (1993).
23. Bos-Mikich, A., Whittingham, D. G. & Kones, K. T. Meiotic and Mitotic Ca^{2+} oscillations affect cell composition in resulting blastocysts. *Dev. Biol.* **182,** 172–179 (1997).
24. Dietrich, W. *et al.* A genetic map of the mouse suitable for typing intraspecific crosses. *Genetics* **131,** 423–447 (1992).
25. Taylor, B. A. & Rowe, L. A mouse linkage testing stock possessing multiple copies of the endogenous ecotropic murine leukemia virus genome. *Genomics* **5,** 221–232 (1989).
26. Johnson, K. R., Cook, S. A. & Davisson, M. T. Chromosomal localization of the murine gene and two related sequences encoding high-mobility-group I and Y proteins. *Genomics* **12,** 503–509 (1992).

Acknowledgements. This study was supported in part by grants from the National Institutes of Health, ProBio America Inc., and fellowships from the Japanese Society for the Promotion of Science (T.W.) and European Molecular Biology Organization (A.C.F.P.). We thank H. Tateno for chromosome analysis, Y. Nakamura for help with DNA fingerprinting, H. Kishikawa, T. Kasai and R. Kleinfeld for assistance in preparing this manuscript, and J. Eppig for help and advice.

Correspondence and requests for materials should be addressed to R.Y.

Defects in somite formation in *lunatic fringe*-deficient mice

Nian Zhang & Thomas Gridley

The Jackson Laboratory, 600 Main Street, Bar Harbor, Maine 04609-1500, USA

Segmentation in vertebrates first arises when the unsegmented paraxial mesoderm subdivides to form paired epithelial spheres called somites[1,2]. The Notch signalling pathway is important in regulating the formation and anterior–posterior patterning of the vertebrate somite[3–7]. One component of the Notch signalling pathway in *Drosophila* is the *fringe* gene, which encodes a secreted signalling molecule required for activation of Notch during specification of the wing margin[8–11]. Here we show that mice homozygous for a targeted mutation of the *lunatic fringe* (*Lfng*) gene, one of the mouse homologues[12,13] of *fringe*, have defects in somite formation and anterior–posterior patterning of the somites. Somites in the mutant embryos are irregular in size and shape, and their anterior–posterior patterning is disturbed. Marker analysis revealed that in the presomitic mesoderm of the mutant embryos, sharply demarcated domains of expression of several components of the Notch signalling pathway are replaced by even gradients of gene expression. These results indicate that *Lfng* encodes an essential component of the Notch signalling pathway during somitogenesis in mice.

The *Lfng* gene is expressed during somitogenesis in mice in a dynamic pattern that suggests a possible role for *Lfng* in regulating somite formation and establishing somite borders[12,13]. To analyse the role of the *Lfng* gene during embryogenesis, we constructed a targeting vector that deleted 0.7 kilobases (kb) of genomic sequence encoding the putative signal peptide and proprotein region of the Lfng protein, and replaced the deleted sequence with the *lacZ* gene of *Escherichia coli* (Fig. 1a, b). Mice heterozygous for the $Lfng^{LacZ}$ mutant allele were viable and fertile. The pattern of RNA expression from the $Lfng^{LacZ}$ mutant allele was identical to that of *Lfng* RNA expression, but expression of β-galactosidase protein from the $Lfng^{LacZ}$ mutant allele was not useful as a marker for visualizing the normal pattern of *Lfng* expression during somitogenesis owing to the perdurance of the β-galactosidase protein and the dynamic nature of the *Lfng* expression pattern (Fig. 1c–e).

At birth, $Lfng^{LacZ}$ homozygous neonates had a shortened trunk with a rudimentary tail (Fig. 2a). Some $Lfng^{LacZ}$ homozygous neonates died within a few hours of birth, apparently from respiratory difficulties due to malformed rib cages (see below), but other, less severely affected, $Lfng^{LacZ}$ homozygotes could survive to adulthood. Analysis of stained skeletal preparations revealed substantial defects in formation of the vertebral column and ribs in the $Lfng^{LacZ}$ homozygotes (Fig. 2b, c). The regular metameric pattern of the vertebrae was disrupted along the entire longitudinal axis. The ribs of the $Lfng^{LacZ}$ homozygotes were bifurcated and fused, and some ribs were detached from the vertebral column (Fig. 2c).

$Lfng^{LacZ}$ homozygous mutant embryos could be distinguished

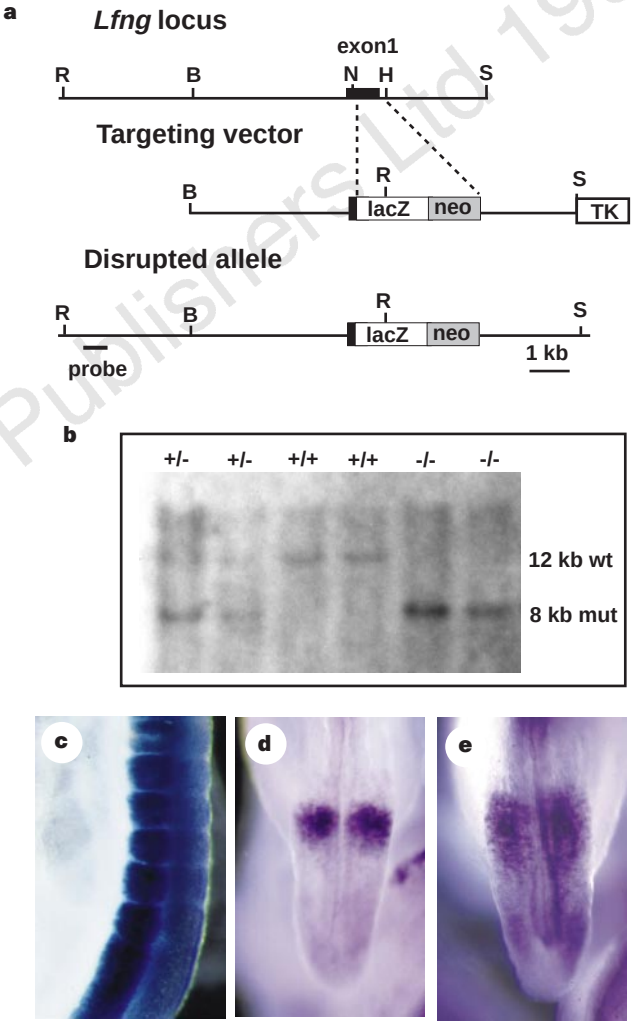

Figure 1 Targeted disruption of the *Lfng* gene. **a**, Targeting scheme. The top line shows the genomic organization of a portion of the *Lfng* gene; the middle line shows the structure of the targeting vector. A 0.7-kb deletion was created which removes most of exon 1, replacing it with the *lacZ* gene and a *neo* cassette. At the bottom is the predicted structure of the *Lfng* locus following homologous recombination of the targeting vector. The probe used for Southern blot analysis in **b** is indicated. Restriction enzymes: B, *Bam*HI; H, *Hin*dIII; N, *Not*I; R, *Eco*RV; S, *Sal*I. **b**, DNA isolated from embryos of the intercross of $Lfng^{LacZ}$/+ heterozygous mice was digested with *Eco*RV, blotted, and hybridized with the indicated probe. Genotypes of progeny are indicated at the top of each lane. **c**, β-Galactosidase expression in $Lfng^{LacZ}$/+ heterozygous embryos revealed that, unlike *Lfng* RNA, β-galactosidase protein was expressed throughout the rostral presomitic mesoderm and the most recently formed somites. **d**, *In situ* hybridization of a $Lfng^{LacZ}$/+ heterozygous embryo with a *lacZ* probe revealed the same banding pattern in the presomitic mesoderm as is observed with a *Lfng* probe, demonstrating that the constitutive expression observed in **c** is due to perdurance of β-galactosidase. **e**, *In situ* hybridization of a $Lfng^{LacZ}$ homozygous mutant embryo with a *lacZ* probe revealed that the stripe of *lacZ* RNA expression is expanded and is more diffuse than in $Lfng^{LacZ}$/+ heterozygous embryos. In **c**–**e**, posterior is at the bottom. **c**, Sagittal view; **d**, **e**, dorsal views.